Wigner-Seitz model of charged lamellar colloidal dispersions

Emmanuel Trizac* and Jean-Pierre Hansen†
Laboratoire de Physique, URA 1325 du CNRS, Ecole Normale Supérieure de Lyon, 69364 Lyon Cedex 07, France
(Received 20 March 1997)

A concentrated suspension of lamellar colloidal particles (e.g., clay) is modeled by considering a single, uniformly charged, finite platelet confined with co- and counterions to a Wigner-Seitz (WS) cell. The system is treated within Poisson-Boltzmann theory, with appropriate boundary conditions on the surface of the WS cell, supposed to account for the confinement effect of neighboring platelets. Expressions are obtained for the free energy, osmotic, and disjoining pressures and the capacitance in terms of the local electrostatic potential and the co- and counterion density profiles. Explicit solutions of the *linearized* Poisson-Boltzmann equation are obtained for circular and square platelets placed at the center of a cylindrical or parallelepipedic cell. The resulting free energy is found to go through a minimum as a function of the aspect ratio of the cell, for any given volume (determined by the macroscopic concentration of platelets), platelet surface charge, and salt concentration. The optimum aspect ratio is found to be nearly independent of the two latter physical parameters. The osmotic and disjoining pressures are found to coincide at the free energy minimum, while the total quadrupole moment of the electric double layer formed by the platelet and the surrounding co- and counterions vanishes simultaneously. The osmotic equation of state is calculated for a variety of physical conditions. The limit of vanishing platelet concentration is considered in some detail, and the force acting between two coaxial platelets is calculated in that limit as a function of their separation. [S1063-651X(97)14508-1]

PACS number(s): 82.70.Dd, 68.10.−m

I. INTRODUCTION

Charge-stabilized colloidal suspensions have been the object of intense theoretical scrutiny, starting with the classic work of Derjaguin and Landau and of Verwey and Overbeek (DLVO) [1], on interacting electric double layers, which took its roots in the even earlier work of Gouy [2] and Chapman [3] on double layers near infinite, uniformly charged planes. Following the latter pioneering contributions, a large body of work has been devoted to the planar geometry, which is relevant for electric double layers near macroscopic electrodes [4] or near membranes of biological interest [5]. DLVO theory applies to spherical geometry in particular, and yields an effective interaction between the electric double layers surrounding spherical colloidal particles, in the form of a screened Coulomb potential, the validity of which has been tested both theoretically [6,7] and experimentally [8]. The cylindrical geometry, appropriate for (infinitely) long, stiff polyelectrolyte chains, has been investigated along similar lines, starting with the work of Fuoss and collaborators [9,10]. The common framework of much of this work is Poisson-Boltzmann (PB) theory, which is a mean-field approximation within the density functional theory of inhomogeneous fluids [11].

Poisson-Boltzmann theory applies equally well to the description of the inhomogeneous distributions of co- and counterions around an isolated charged colloidal particle (or polyion) suspended in an ionic solution, and to a concentrated suspension of polyions, provided the ''cage'' of neighboring polyions is modeled by a Wigner-Seitz (WS) cell of appropriate geometry, to which each polyion is confined. Given proper boundary conditions, the Wigner-Seitz model reduces the initial many-polyion suspension to the much simpler problem of a single polyion confined with its associated co- and counterions to a cell of volume equal to the volume per polyion of the dispersion. The shape of the WS cell should reflect the shape of the polyion: It will be an infinite slab for a membrane [5], an infinite coaxial cylinder in the case of a linear polyelectrolyte [9], or a concentric sphere surrounding a spherical colloid [12].

Except in the case of spheres, the aforementioned models and calculations deal with the case of polyions of infinite extension (e.g., an infinite plane in the case of membranes or an infinite line or cylinder in the case of polyelectrolyte chains). In this paper, we examine the case of rigid membranes or platelets of finite size. Restriction will be made to infinitely thin, uniformly charged circular or square platelets. These may be considered as a reasonable model for dispersions of smectite clay particles, like the natural montmorillonite clays [13] or the synthetic Laponite clays [14]. While the former are irregularly shaped polygonal particles, the latter are, to a good approximation, of a circular shape (disklike particles). The thickness of a real clay particle is of the order of 1 nm, which is much less than lateral dimensions (Laponite disks have a diameter of typically 25 nm), so that the picture of infinitely thin platelets is acceptable. The main difficulty in a statistical description of such platelets lies in the considerable anisotropy of the particles and of their associated electric double layers, compared to the much-studied case of spherical colloids.

The main objective of this paper is to obtain expressions for the density profiles of co- and counterions around a circular or square platelet of finite size, confined to WS cells of cylindrical or parallelepipedic geometry. The calculations are carried out within linearized Poisson-Boltzmann theory, and the calculated profiles and potential distributions will be used

*Electronic address: etrizac@physique.ens-lyon.fr
†Electronic address: hansen@physique.ens-lyon.fr

to evaluate key equilibrium properties of concentrated lamellar suspensions, including the free energy, the stress tensor, the capacitance, and the quadrupole moment of a platelet and its associated electric double layer.

Preliminary accounts of parts of this work have appeared elsewhere [15–17].

II. DENSITY FUNCTIONAL AND POISSON-BOLTZMANN THEORY

It is instructive to repeat the derivation of the familiar Poisson-Boltzmann equation from the free energy functional of the inhomogeneous fluid of co- and counterions contained in a WS cell, and subjected to the electric field due to the uniform charge density on the finite platelet placed at the center of the WS cell. In the case of smectite clays, the surface charge density $\sigma=-Ze/\Sigma_p$ (where Σ_p is the area of the platelet and $-Ze$ the total charge, in multiples of the proton charge $e>0$) is negative, so that the counterions are positive, while the co-ions are negative; both are assumed to be monovalent. The local co- and counterion densities (or density profiles) are denoted by $\rho^-(\mathbf{r})$ and $\rho^+(\mathbf{r})$, where $\mathbf{r}$ is a position vector pointing inside the WS cell. If N^+ and N^- are the total numbers of co- and counterions inside the WS cell, the $\rho^\alpha(\mathbf{r})$ satisfy the normalization condition

$$\int_\Omega \rho^\alpha(\mathbf{r})d^3\mathbf{r}=N^\alpha, \quad \alpha=+,-, \tag{1}$$

where Ω is the volume of the WS cell, which is equal to the average volume per platelet in the colloidal suspension. Overall charge neutrality requires that

$$N^+-N^--Z=0. \tag{2}$$

The free energy functional $\mathcal{F}[\rho^+,\rho^-]$ may be split into the usual ideal, Coulombic, and correlational contributions [11]:

$$\mathcal{F}=\mathcal{F}_{\rm id}+\mathcal{F}_{\rm Coul}+\mathcal{F}_{\rm corr}, \tag{3}$$

with

$$\mathcal{F}_{\rm id}[\{\rho^\alpha\}]=k_BT\sum_{\alpha=+,-}\int_\Omega d^3\mathbf{r}\rho^\alpha(\mathbf{r})[\ln(\Lambda_\alpha^3\rho^\alpha(\mathbf{r}))-1],$$

$$\mathcal{F}_{\rm Coul}[\{\rho^\alpha\}]=\frac{1}{2}\int_\Omega\{q_{\mathcal{P}}(\mathbf{r})+e[\rho^+(\mathbf{r})-\rho^-(\mathbf{r})]\}\varphi(\mathbf{r})d^3\mathbf{r}.$$

In these equations, Λ_α is the de Broglie thermal wavelength of ions of species α; $q_{\mathcal{P}}(\mathbf{r})$ denotes the (surface) charge density of the platelet and $\varphi(\mathbf{r})$ is the total electrostatic potential at $\mathbf{r}$, which satisfies Poisson's equation

$$\nabla^2\varphi(\mathbf{r})=-\frac{4\pi}{\varepsilon}q_{\mathcal{P}}(\mathbf{r})-\frac{4\pi e}{\varepsilon}[\rho^+(\mathbf{r})-\rho^-(\mathbf{r})]. \tag{4}$$

In the above expression, ε is the dielectric constant of the solvent (generally water) regarded as a continuous medium (''primitive model''). The correlation part $\mathcal{F}_{\rm corr}$ is not known explicitly, but may be expressed within the local density approximation [11,6]. $\mathcal{F}_{\rm corr}$ will be neglected throughout, an approximation which is reasonable, as long as the local concentrations of co- and counterions are not too high, a condition which may not be fulfilled for the counterions in the immediate vicinity of a highly charged platelet. For a complete formulation of the electrostatic problem, the form (3) of the free energy functional must be supplemented by specifying the boundary conditions satisfied by the resulting mean electrostatic potential, or its gradient, on the surface Σ of the WS cell.

The equilibrium density profiles $\rho^\alpha(\mathbf{r})$ are those which minimize the free energy functional (3), subject to the constraints (1), i.e.,

$$\frac{\delta\mathcal{F}[\rho^+,\rho^-]}{\delta\rho^\alpha(\mathbf{r})}=\mu_\alpha,\alpha=+,-, \tag{5}$$

where μ_α is the Lagrange multiplier associated with the constraint (1), i.e., the chemical potential of species α. The functional derivative of the Coulombic term $\mathcal{F}_{\rm coul}$ reads

$$\frac{\delta\mathcal{F}_{\rm coul}}{\delta\rho^\pm(\mathbf{r})}=\pm e\varphi(\mathbf{r}). \tag{6}$$

With $\mathcal{F}_{\rm corr}=0$, the functional derivatives are easily calculated and the optimum density profiles are found to be given by the Boltzmann distribution

$$\rho^\pm(\mathbf{r})=\rho_0^\pm\exp\{\mp\beta e\varphi(\mathbf{r})\}, \tag{7}$$

where $\beta=1/(k_BT)$ is the inverse temperature in energy units.

For a given $q_{\mathcal{P}}(\mathbf{r})$, Eqs. (4) and (7) form a closed set, which may be reexpressed as an inhomogeneous nonlinear partial differential equation for the potential $\varphi(\mathbf{r})$, usually referred to as the Poisson-Boltzmann (PB) equation:

$$\nabla^2\varphi(\mathbf{r})+\frac{4\pi e}{\varepsilon}[\rho_0^+\exp\{-\beta e\varphi(\mathbf{r})\}-\rho_0^-\exp\{+\beta e\varphi(\mathbf{r})\}]$$

$$=-\frac{4\pi}{\varepsilon}q_{\mathcal{P}}(\mathbf{r}). \tag{8}$$

Neglect of $\mathcal{F}_{\rm corr}$ clearly points to the mean-field nature of PB theory. The prefactors $\rho_0^\pm$ are equal to the fugacities $\exp(\beta\mu_\pm)/\Lambda_\pm^3$ in the case of an open system, where the WS cell is in equilibrium with an infinite reservoir which fixes the chemical potentials $\mu_\pm$. For a suspension of fixed ionic composition (canonical ensemble), the $\rho_0^\pm$ are determined from the normalization conditions (1). Equation (8) must be solved, subject to appropriate boundary conditions on the surface Σ of the WS cell. If the surface is regarded as a boundary between WS cells associated with nearest-neighbor platelets, it is natural to impose that the *normal* component of the electric field $\mathbf{E}=-\nabla\varphi$ vanish at each point on Σ. In practice, the homogeneous version of the PB equation (8) is solved for all positions $\mathbf{r}$ outside the platelet ($\mathbf{r}\notin\Sigma_p$), and the usual discontinuity of the normal component of the field upon crossing the uniformly charged surface Σ_p is taken into account.

The PB equation has been solved numerically for circular platelets of finite thickness (i.e., coinlike cylinders), carrying a positive edge charge, in the limit of an infinitely dilute

suspension ($\Omega\to\infty$) [18]. In this case, the boundary Σ of the WS cell is pushed out to infinity, the electrostatic potential $\varphi(\mathbf{r})$ can be chosen to vanish when $|\mathbf{r}|\to\infty$, and the prefactors $\rho_0^{\pm}$ reduce to the macroscopic co- and counterion number concentrations n^- and n^+ ($n^+=n^-$). An analytic solution of the PB equation (8), for vanishing or finite platelet concentration $n=1/\Omega$, is available only in the limit of an infinite platelet in a WS slab; this geometry reduces the problem to the classic one-dimensional Gouy-Chapman problem [2,3]. For finite platelets, analytic solutions can be obtained only upon linearization of the PB equation (8). For this purpose, it is convenient to redefine the prefactors $\rho_0^{\pm}$ such that

$$\rho^{\pm}(\mathbf{r})=\rho_0^{\pm}\exp\{\mp\beta e[\varphi(\mathbf{r})-\varphi^*]\}, \tag{9}$$

where φ^* is a reference potential to be specified. The resulting linearized PB equation reads

$$\nabla^2\varphi(\mathbf{r})-\kappa_D^2[\varphi(\mathbf{r})-\gamma_0]=-\frac{4\pi}{\varepsilon}q_{\mathcal{P}}(\mathbf{r}), \tag{10}$$

where the squared inverse Debye length $\kappa_D^2=1/\lambda_D^2$ and the constant γ_0 are given by

$$\kappa_D^2=4\pi\ell_B(\rho_0^+ +\rho_0^-), \tag{11a}$$

$$\gamma_0=(\rho_0^+-\rho_0^-)\frac{4\pi e}{\varepsilon\kappa_D^2}+\varphi^*=\frac{kT}{e}\frac{\rho_0^+-\rho_0^-}{\rho_0^+ +\rho_0^-}+\varphi^*, \tag{11b}$$

and $\ell_B=\beta e^2/\varepsilon$ is the Bjerrum length ($\ell_B\simeq 0.7$ nm in water at room temperature). The normalization conditions (1) now reduce to

$$n^{\pm}=\frac{N^{\pm}}{\Omega}=\rho_0^{\pm}[1\pm\beta e(\varphi^*-\overline{\varphi})], \tag{12}$$

where $\overline{\varphi}$ is the mean potential in the WS cell:

$$\overline{\varphi}=\frac{1}{\Omega}\int_\Omega\varphi(\mathbf{r})d^3\mathbf{r}. \tag{13}$$

A particularly simple choice is thus to linearize the local densities around $\overline{\varphi}$, i.e., to take $\varphi^*=\overline{\varphi}$ [16], in which case

$$\rho_0^{\pm}=n^{\pm}\quad\text{and}\quad\kappa_D^2=4\pi\ell_B(n^+ +n^-). \tag{14}$$

It is worthwhile to note that linearized Poisson-Boltzmann (LPB) theory may be derived from the free energy functional (3) (with $\mathcal{F}_{\rm corr}=0$) via the variational principle (5), provided the integrand in the ''ideal'' contribution $\mathcal{F}_{\rm id}$ is expanded to second order in powers of the local densities $\rho^\alpha(\mathbf{r})$ from their mean n^α [6].

Before turning to the presentation of explicit solutions of LPB theory for specific geometries, we address the problem of expressing and calculating key macroscopic quantities like the free energy, the stress tensor, and the osmotic pressure, from the density profiles.

III. FREE ENERGY AND PRESSURE TENSOR

The Helmholz free energy F of the electric double layer around a colloidal particle inside a WS cell is the key thermodynamic quantity which must be evaluated with care [1,5,19]. Within mean-field PB theory, the free energy F may, in principle, be calculated by substituting the equilibrium density profiles $\rho^\alpha(\mathbf{r})$, determined via the variational principle (5), into the functional (3) (with $\mathcal{F}_{\rm corr}=0$). This expression of the free energy may be cast in the standard form

$$F=U-TS, \tag{15}$$

where the internal energy and the entropy are given by [16]

$$\begin{aligned}U&=\frac{1}{2}\int_\Omega\{q_{\mathcal{P}}(\mathbf{r})+e[\rho^+(\mathbf{r})-\rho^-(\mathbf{r})]\}\varphi(\mathbf{r})d^3\mathbf{r}\\&=\frac{\varepsilon}{8\pi}\int_\Omega[\nabla\varphi(\mathbf{r})]^2d^3\mathbf{r}-\frac{\varepsilon}{8\pi}\oint_\Sigma\varphi(\mathbf{r})\nabla\varphi(\mathbf{r})\cdot d\mathbf{S}\end{aligned} \tag{16}$$

and

$$\begin{aligned}TS&=-k_BT\sum_{\alpha=+,-}\int_\Omega\rho^\alpha(\mathbf{r})[\ln(\Lambda_\alpha^3\rho^\alpha(\mathbf{r}))-1]d^3\mathbf{r}\\&=-k_BT\sum_{\alpha=+,-}N^\alpha\ln(\rho_0^\alpha\Lambda_\alpha^3)+\int_\Omega\{e[\rho^+(\mathbf{r})-\rho^-(\mathbf{r})]\\&\quad\times\varphi(\mathbf{r})+k_BT[\rho^+(\mathbf{r})+\rho^-(\mathbf{r})]\}d^3\mathbf{r}.\end{aligned} \tag{17}$$

In Eqs. (16) and (17), the $\rho^\alpha(\mathbf{r})$ are the equilibrium profiles, and use was made of Eqs. (4) and (7) in going from the first to the second line in each of these equations. The resulting expression for the dimensionless free energy βF reads, in terms of the dimensionless electrostatic potential $\Phi(\mathbf{r})=\beta e\varphi(\mathbf{r})$,

$$\begin{aligned}\beta F&=\sum_{\alpha=+,-}N^\alpha\ln(\rho_0^\alpha\Lambda_\alpha^3)-\frac{1}{8\pi\ell_B}\oint_\Sigma\Phi(\mathbf{r})\nabla\Phi(\mathbf{r})\cdot d\mathbf{S}\\&\quad+\int_\Omega\Big\{[\rho^-(\mathbf{r})-\rho^+(\mathbf{r})]\Phi(\mathbf{r})-[\rho^+(\mathbf{r})+\rho^-(\mathbf{r})]\\&\quad+\frac{1}{8\pi\ell_B}[\nabla\Phi(\mathbf{r})]^2\Big\}d^3\mathbf{r}.\end{aligned} \tag{18}$$

Expression (18), valid within the nonlinear PB approximation, involves integrations over the WS boundary surface (which do not contribute if the boundary condition of vanishing normal electric field is adopted) and over the volume of the WS cell, and is hence not very tractable. Equivalent expressions for the free energy can be obtained by considering generic charging processes [1,5,16,19]. For a fixed cell geometry (volume and shape), the variation in free energy due to infinitesimal variations of the potential $[\Phi(\mathbf{r})\to\Phi(\mathbf{r})+\delta\Phi(\mathbf{r})]$ and of the Bjerrum length ($\ell_B\to\ell_B+\delta\ell_B$) is of the generic form [16]

$$\delta(\beta F)=\frac{1}{8\pi\ell_B}\oint_\Sigma[\Phi\nabla(\delta\Phi)-\delta\Phi\nabla\Phi]\cdot d\mathbf{S}+\beta U\frac{\delta\ell_B}{\ell_B}+\int_{\Sigma_p}\Phi\,\delta\left(\frac{\sigma}{e}\right)d^2\mathbf{r}+[\ln(\rho_0^+\Lambda_+^3)]\delta N_+ +[\ln(\rho_0^-\Lambda_-^3)]\delta N_-, \tag{19}$$

where $\sigma=-Ze/\Sigma_p$ is the surface charge of a platelet per unit area. Expressions of the free energy can be derived from Eq. (19) by considering various real or virtual charging processes. In practice, we have calculated F using a constant Debye length charging process, from a situation where the platelet is neutral ($Z'=0$) to its final charge ($Z'=Z$). For uncharged platelets, $N_0^+=N_0^-=N_0=\Omega n_s+Z/2$, where n_s is the salt concentration. At any stage of the process, $N^\pm=N_0\pm Z'/2$, and Eq. (19) shows that in an infinitesimal step, during which the boundary condition of vanishing normal electric field is enforced, the free energy changes by

$$\beta\delta(F)=\int_{\Sigma_p}\Phi\,\delta\left(\frac{\sigma}{e}\right)d^2\mathbf{r}+[\ln(\rho_0^+\Lambda_+^3)]\delta N_+ +[\ln(\rho_0^-\Lambda_-^3)]\delta N_-. \tag{20}$$

Integration along this path yields

$$F(\sigma)-F(\sigma=0)=\int_0^\sigma\left[\int_{\Sigma_p}\varphi^{\sigma'}(\mathbf{r})d^2\mathbf{r}\right]d\sigma' +N_0kT\ln\left\{\frac{(N_0)^2-Z^2/4}{(N_0)^2}\right\} +\frac{Z}{2}kT\ln\left\{\frac{N_0+Z/2}{N_0-Z/2}\right\}. \tag{21}$$

The result (19), valid for a given WS cell geometry, may be generalized to the case of an infinitesimal change $\delta\Omega$ of the geometry (shape and/or volume) of the cell. A calculation given in the Appendix shows that for fixed numbers of co- and counterions (N^+ and N^-) in the cell, the resulting infinitesimal change in free energy reads

$$\delta F=-k_BT\sum_{\alpha=+,-}\int_{\delta\Omega}\rho^\alpha(\mathbf{r})d^3\mathbf{r}-\frac{\varepsilon}{8\pi}\int_{\delta\Omega}[\nabla\varphi]^2d^3\mathbf{r}, \tag{22}$$

where it has been assumed that the electric field has no normal component on the WS surface. Under these circumstances, the previous expression for δF is compatible with the usual definition of the pressure tensor in a charged medium [20],

$$\overleftrightarrow{\Pi}=\left[P(\mathbf{r})+\frac{\varepsilon}{8\pi}(\boldsymbol{E})^2\right]\overleftrightarrow{I}-\frac{\varepsilon}{4\pi}\mathbf{E}(\mathbf{r})\otimes\mathbf{E}(\mathbf{r}), \tag{23}$$

where $\mathbf{E}(\mathbf{r})=-\nabla\varphi(\mathbf{r})$, and for noninteracting ions,

$$P(\mathbf{r})=k_BT\sum_{\alpha=+,-}\rho^\alpha(\mathbf{r}). \tag{24}$$

The compatibility of Eqs. (22) and (23) plus Eq. (24) is easily verified by considering a small local volume change $\delta\Omega$ due to the displacement by an amount $\delta\ell$ of a small area element $\delta\boldsymbol{\Sigma}$ at the surface of the WS cell. The pressure tensor (23) satisfies the mechanical equilibrium condition

$$\boldsymbol{\nabla}\cdot\overleftrightarrow{\boldsymbol{\Pi}}(\mathbf{r})=\mathbf{0}, \tag{25}$$

which, upon substitution of Eq. (23) into Eq. (25), and use of Poisson's equation (4), is equivalent to the familiar force balance equation

$$\nabla P(\mathbf{r})=e[\rho^+(\mathbf{r})-\rho^-(\mathbf{r})]\mathbf{E}(\mathbf{r}). \tag{26}$$

There is no obvious definition of the macroscopic osmotic pressure of the co- and counterions within the present WS model. An element $d\mathbf{S}$ of the surface of the WS cell is subjected to the force:

$$d\mathbf{F}=\overleftrightarrow{\Pi}\cdot d\mathbf{S}=\left(k_BT\sum_{\alpha=+,-}\rho^\alpha+\frac{\varepsilon}{8\pi}E^2\right)d\mathbf{S}. \tag{27}$$

It is hence tempting to define the osmotic pressure as

$$\Pi=k_BT\sum_{\alpha=+,-}\overline{\rho^\alpha}^\Sigma+\frac{\varepsilon}{8\pi}\overline{E^2}^\Sigma, \tag{28}$$

where the averages are taken over the total surface bounding the WS cell. The same expression for Π follows from the volume derivative of the free energy, for a particular infinitesimal dilation of the WS cell. The latter is chosen such that for each surface element dS of the WS cell, the infinitesimal volume element is $d\Omega=d\Sigma\,\delta\ell$, where $\delta\ell$ is a constant displacement along the normal to $d\Sigma$. Under these conditions, we deduce from Eq. (22) that

$$\delta F=-k_BT\delta\ell\sum_{\alpha=+,-}\oint_\Sigma\rho^\alpha(\mathbf{r})d\Sigma-\frac{\varepsilon}{8\pi}\delta\ell\oint_\Sigma(\nabla\varphi)^2d\Sigma, \tag{29}$$

so that

$$\frac{\partial F}{\partial\Omega}=\lim_{\delta\ell\to0}\frac{\delta F}{\Sigma\,\delta\ell}=-k_BT\overline{\rho^\alpha}^\Sigma-\frac{\varepsilon}{8\pi}\overline{[(\nabla\varphi)^2]}^\Sigma=-\Pi. \tag{30}$$

Similarly, one may express the disjoining pressure Π_d (i.e., the pressure to be applied to maintain the parallel platelets of a stack at a distance H which coincides with the height of the WS cell) by considering the variation of the free energy (22) upon increasing H by an infinitesimal amount δH; the corresponding increase in the volume of the WS cell is $\delta\Omega=S\,\delta H$, where S is the cross section of the cell parallel to the platelet (cf. the prismatic geometries considered in the following sections). By proceding as in the case of the osmotic pressure, one arrives at the required expression

$$\Pi_d=-\frac{\partial(F/S)}{\partial H}=k_BT\overline{\rho^\alpha}^S+\frac{\varepsilon}{8\pi}\overline{[(\nabla\varphi)^2]}^S=\overline{\Pi_{zz}}^S, \tag{31}$$

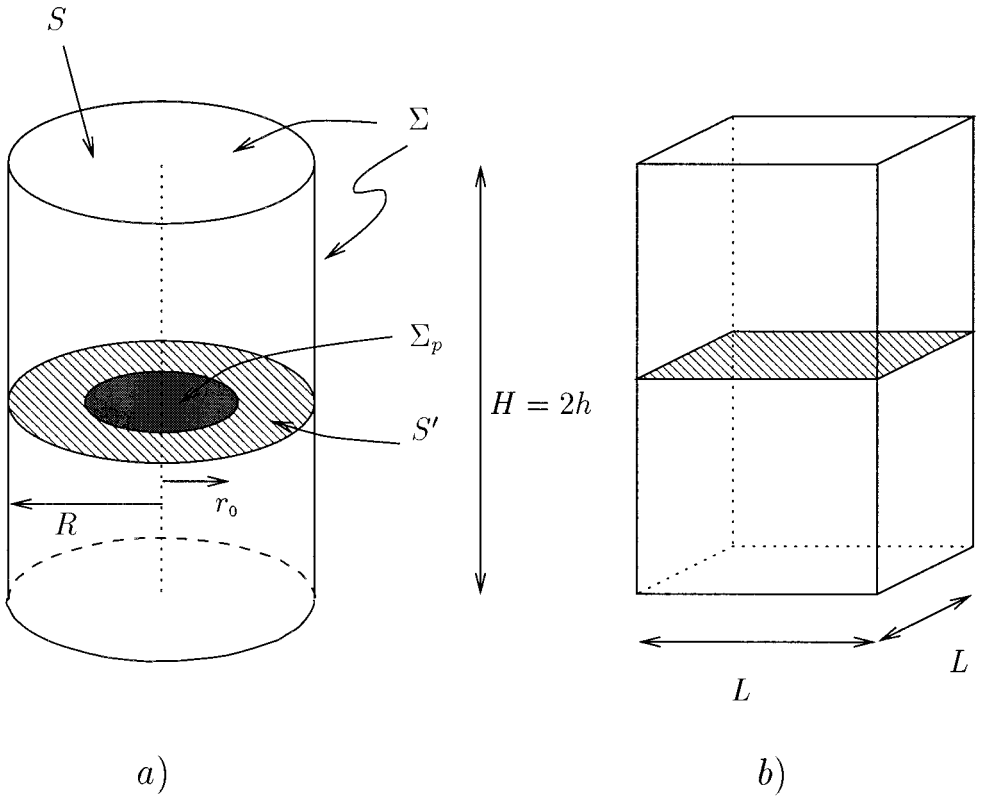

FIG. 1. The prismatic cells considered in this paper. (a) shows a circular platelet in a cylindrical cell, whereas (b) represents the parallelepipedic cell containing either a circular or a square platelet lying in the dashed region S'.

where the average is now taken over the cross section S, i.e., on the surface of the WS cell parallel to the platelet, and the normal to the platelet is chosen along the z axis. Π_d is thus related to the mean uniaxal stress along the normal to the platelets.

Another instructive quantity is the capacitance C of the electric double layer associated with a platelet. For finite platelets, the definition of C is ambiguous. We define the capacitance in terms of the difference $(\Delta\overline{\varphi})^{S'-S}=\overline{\varphi}^{S'}-\overline{\varphi}^{S}$ between the potential averaged over the cross section S' of the cell containing the platelet $(z=0)$, and the corresponding average on the surface S midway between two platelets in a stack ($z=H/2$; cf. Fig. 1 for the case of cylindrical and parallelepipedic WS cells). The capacitance is thus defined by

$$C(\Delta\overline{\varphi})^{S'-S}=\sigma. \tag{32}$$

The reciprocal of the capacitance defines a length $\lambda_c=C^{-1}$ which characterizes the thickness of the electric double layer.

The total charge inside a WS cell is zero, and due to space reflection symmetry, the electric dipole moment associated with the charge distribution inside the cell vanishes. The first *a priori* nonvanishing multipole moment of the charge distribution is the quadrupole moment $Q=Q_{zz}=-2Q_{xx}=-2Q_{yy}$:

$$Q_{zz}^{\mathrm{tot}}=\frac{1}{2}\int_{\Omega}\{q_{\mathcal{P}}(\mathbf{r})+e[\rho^{+}(\mathbf{r})-\rho^{-}(\mathbf{r})]\}(2z^2-x^2-y^2)d^3\mathbf{r}. \tag{33}$$

In the two following sections, the quantities defined in this section will be calculated within cylindrical and parallelepipedic geometries, for disk-shaped and square platelets.

IV. CYLINDRICAL GEOMETRY

We consider first the case of disk-shaped platelets, of radius r_0. In Ref. [15] explicit solutions of LPB theory were obtained in terms of infinite series of Legendre or Bessel functions, for spherical and cylindrical WS cells. We reexamine the latter geometry in some detail here. The cylindrical WS cell is of radius R and of height $H=2h$ (cf. Fig. 1), so that $\Omega=2\pi R^2h$. The electrostatic potential within the WS cell is a function $\varphi(r,z)$ of the cylindrical coordinates r and z, which satisfies the boundary conditions

$$\left.\frac{\partial\varphi(r,z)}{\partial r}\right|_{r=R}=0, \tag{34a}$$

$$\left.\frac{\partial\varphi(r,z)}{\partial z}\right|_{z=\pm h}=0. \tag{34b}$$

Since these conditions, as well as the discontinuity of the electric field $E_z(z=0^{\pm})=-(\partial\varphi/\partial z)_{z=0^{\pm}}$ across the disk $(r<r_0)$, involve only the derivatives of the potential, one may assume $\overline{\varphi}=0$ without loss of generality [cf. Eq. (13)]. Under these conditions, the solution of the linearized PB equation (10) may be expanded in a Bessel-Dini series [15]:

$$\varphi(r,z)=\sum_{n=1}^{\infty}A_n(z)J_0\left(y_n\frac{r}{R}\right), \tag{35}$$

where y_n is the n^{th} root of $J_1(y)\equiv-dJ_0(y)/dy=0$, and J_0 and J_1 are the Bessel functions of zeroth and first order $(y_1=0)$. The resulting differential equations for the coefficients $A_n(z)$ are easily solved, leading to the final result

$$\Phi(r,z)=\beta e\varphi(r,z)=\beta e\gamma_0+\frac{1}{\kappa_D b}\left(\frac{r_0}{R}\right)^2\frac{\cosh[\kappa_D(h-|z|)]}{\sinh(\kappa_D h)}$$
$$+\frac{2}{b}\frac{r_0}{R}\sum_{n=2}^{\infty}\frac{\Lambda_n J_1(k_n r_0)}{y_n\sinh(h/\Lambda_n)J_0^2(y_n)}$$
$$\times\cosh\left(\frac{h-|z|}{\Lambda_n}\right)J_0(k_n r), \tag{36}$$

where $b=e/(2\pi\ell_B\sigma)$ is the Gouy length, $\Lambda_n=R/\sqrt{y_n^2+\kappa_D^2R^2}$, and $k_n=y_n/R$.

For any given macroscopic density of platelets, n, and hence a given volume $\Omega=1/n$ of the WS cell, only the product R^2h is fixed. Since R cannot be less than the disk radius r_0, the aspect ratio $h/r_0\leqslant(2\pi nr_0^3)^{-1}$. At the upper limit of this range, i.e., for $R=r_0$, and with the chosen boundary conditions, the electrostatic problem reduces to that of an infinite uniformly charged plane in a WS slab of width $H=2h$. With $R=r_0$ the potential in Eq. (36) indeed reduces to the first two terms, which are independent of the radial coordinate r, i.e.,

$$\lim_{R\to r_0}\Phi(r,z)=\Phi(z)=\beta e\gamma_0+\frac{1}{\kappa_D b}\frac{\cosh[\kappa_D(h-|z|)]}{\sinh(\kappa_D h)}. \tag{37}$$

The above expression is precisely the solution of the one-dimensional LPB equation for an infinite uniformly charged plane in a slab, and the familiar result $\Phi(z)=\exp(-\kappa_D z)/(\kappa_D b)$ is recovered when $h\to\infty$.

The density profiles calculated from the potential (36) via Eq. (9) are sensitive to the aspect ratio h/r_0 for a given cell volume Ω. The ''optimum'' ratio is determined by minimizing the free energy F with respect to this ratio. F is calculated via the constant Debye length charging process, resulting in Eq. (21). The part of that expression which depends on the ratio h/r_0 for a given cell volume is

$$A=\int_0^{\sigma}\left[\int_{\Sigma_p}\varphi^{\sigma'}(r,z=0)d^2\mathbf{r}\right]d\sigma'$$
$$=2\pi\int_0^{\sigma}\left[\int_0^{r_0}\varphi_0^{\sigma'}(r)r\,dr\right]d\sigma'=\pi\sigma\int_0^{r_0}\varphi_0^{\sigma}(r)r\,dr \tag{38}$$

where $\varphi_0(r)\equiv\varphi(r,z=0)$ is the electrostatic potential on the disk and the last line holds within the LPB approximation only, where the potential can always be expressed in the form $\varphi^{\sigma}(\mathbf{r})=\sigma f(\kappa_D,\mathbf{r})$. Substitution of Eq. (36) (with $z=0$) into Eq. (38) yields

$$\frac{\beta}{Z}A=\frac{1}{2}\beta e\gamma_0-\frac{1}{2\kappa_D b}\left\{\left(\frac{r_0}{R}\right)^2\frac{1}{\tanh(\kappa_D h)}\right.$$
$$\left.+4\sum_{n=2}^{\infty}\frac{\kappa_D\Lambda_n J_1^2(k_n r_0)}{y_n^2J_0^2(y_n)\tanh(h/\Lambda_n)}\right\}. \tag{39}$$

An example of the variation of F with h/r_0 is shown in Fig. 2(a). In this example, as well as under all physical conditions that were investigated, F goes through a minimum for a ratio h/r_0, such that the physical requirement that $R>r_0$ is satisfied. Moreover, the location of the minimum turns out to be practically independent of the charge density σ carried by the disk, and of the salt concentration n_s; in other words, the ratio h/r_0 depends ''only'' on the WS cell volume Ω or, equivalently, on the macroscopic density of platelets n. For any density n, the system selects an optimal ratio h/r_0. The variation of this ratio with n in shown in Fig. 3. All figures correspond to $\varepsilon_{\mathrm{CGS}}=78$ and $T=300$ K.

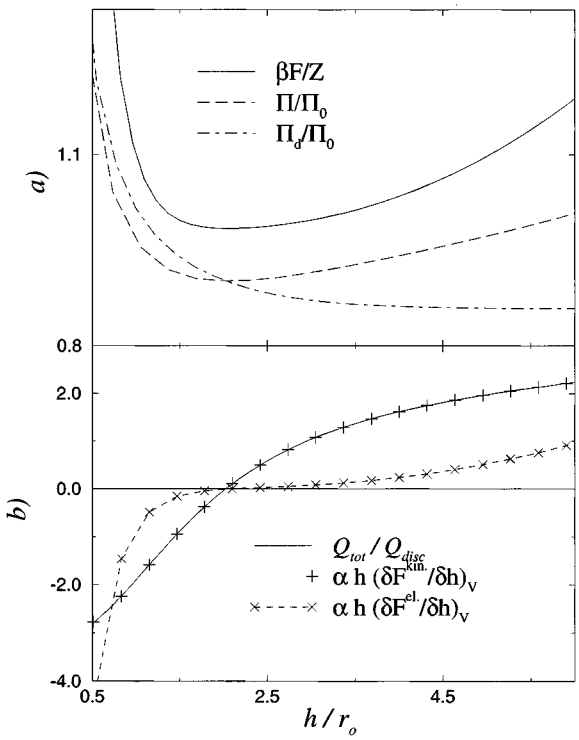

FIG. 2. Variations of the free energy F, the osmotic pressure Π, and the disjoining pressure Π_d with the aspect ratio [upper curves, part (a)]. For illustrative purposes, the free energy has been shifted by an arbitrary constant along the vertical axis. Also shown is the total normalized quadrupole [lower part, (b)]. The kinetic and electrostatic parts of the free energy variation are defined in the appendix [cf Eqs. (A12a) and (A12b)]. In order to check the validity of Eq. (A15), we choose $\alpha^{-1}=\gamma_0\kappa_D^2Q_{zz}^{\mathrm{disk}}/2$. The normalization pressure Π_0 is defined with the macroscopic concentrations of co- and counterions inside the cell: $\Pi_0=k_BT(\rho_0^+ +\rho_0^-)$. The data shown correspond to a circular platelet in a cylindrical cell, with $n_s=10^{-3}M$, $n=10^{-5}M$, and $Z=100$.

The potential $\varphi(r,z)$ and the resulting charge density profile are highly anisotropic functions, as expected from the platelet geometry. This requires that a large number of terms (typically 50–400) be retained in the expansion (36) to ensure adequate convergence. A typical example of equipotential lines is shown in Fig. 4.

If n_s' is the salt concentration in a reservoir which is in osmotic equilibrium with the colloidal suspension, i.e., with the co- and counterions inside the WS cell, then the salt concentration n_s inside the latter is, within LPB theory, related to n_s' by [15]

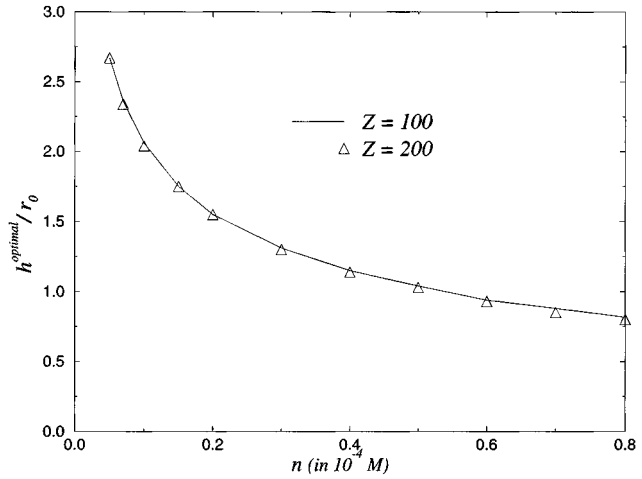

FIG. 3. Variation of the optimal aspect ratio minimizing the free energy with clay concentration, for $n_s' = 10^{-3} M$.

$$\frac{n_s}{n_s'} = \sqrt{1 + \frac{Z^2 n^2}{4(n_s')^2}} - \frac{Zn}{2n_s'} \leqslant 1, \tag{40}$$

which is an expression of the familiar Donnan effect.

The values of the potential and its gradient on the surface Σ of the WS cell may be used to compute the pressures Π and Π_d, according to Eqs. (28) and (31). For a given WS cell volume Ω, the variations of Π and Π_d with the ratio h/r_0 differ: Π_d decreases monotonously as h/r_0 increases, while Π goes through a minimum for h/r_0 close to the ''optimum'' value minimizing the free energy (cf. Fig. 2). At the minimum of the free energy, the two pressures are seen to coincide ($\Pi = \Pi_d$). Taking into account the conservation of the overall volume $\delta(R^2 h) = 0$, Eq. (22) can indeed be rewritten as

$$\delta F = \Sigma \frac{R}{2} \frac{\delta h}{h} [\Pi - \Pi_d], \tag{41}$$

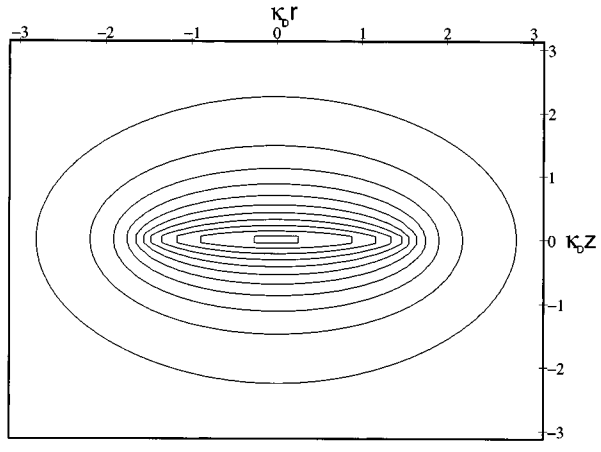

FIG. 4. Equipotential lines in the plane $(\kappa_D r, \kappa_D z)$, with arithmetic spacing between the isopotentials ($\beta e \Delta\varphi = 0.5$ between two succesive curves). Here, $Z = 100$, $n = 10^{-5} M$, and $n_s = 10^{-3} M$. For these parameters, the optimal aspect ratio is $h/r_0 \simeq 2.0$. The reduced radii of the disk and cylinder are, respectively, $\kappa_D r_0 \simeq 1.59$ and $\kappa_D R \simeq 4.14$. The summation in Eq. (36) was truncated after $n_{\max} = 50$.

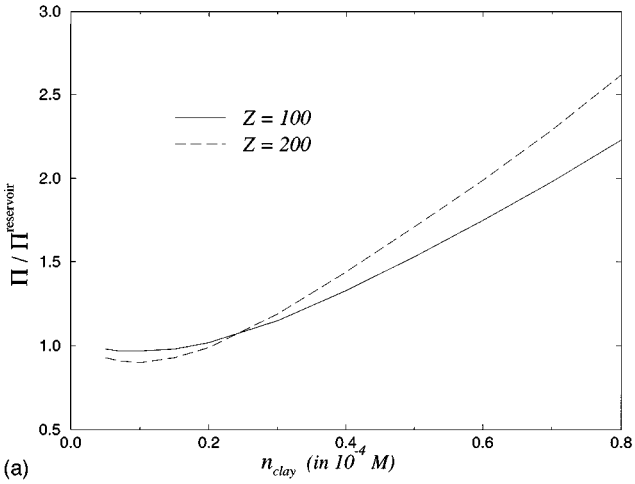

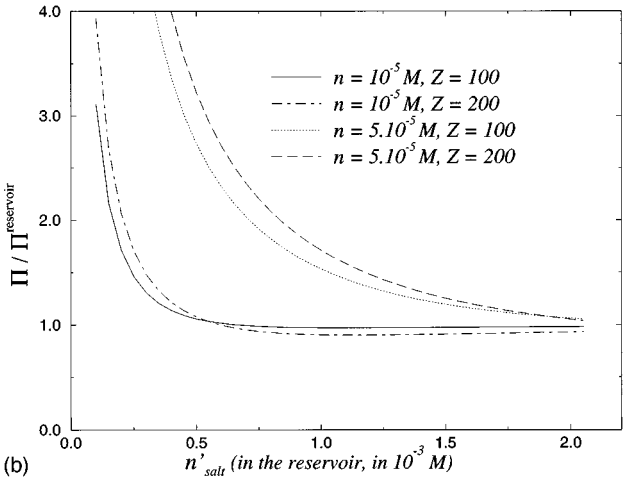

FIG. 5. (a) Clay concentration dependence of the osmotic and disjoining pressures, evaluated at the optimal aspect ratio minimizing the free energy (where $\Pi = \Pi_d$). The salt concentration in the reservoir is held constant ($n_s' = 10^{-3} M$) and defines the normalization pressure $\Pi^{\text{reservoir}} = 2 k_B T n_s'$. (b) Variation of the osmotic and disjoining pressures with the salt concentration in the reservoir (n_s'). For $n_s' \to 0$, Π/Π^{res} diverges like $1/n_s'$, while $\Pi \to$ const.

so that the extremum condition $\delta F = 0$ implies $\Pi = \Pi_d$. The variation of $\Pi = \Pi_d$ with the platelet concentration n and with the salt concentration is shown in Figs. 5(a) and 5(b) for two values of the platelet charge ($Z = 100$ and $Z = 200$). After a shallow minimum, the pressure Π is found to increase with n (for fixed n_s' in the reservoir), whereas it drops rapidly with increasing n_s', towards the value of the osmotic pressure in the reservoir. These tendencies are reminiscent of the experimental and numerical results of Dubois and coworkers concerning lamellar phases of ''infinite'' charged bilayers [22].

The potential distribution may be used to evaluate the capacity C from Eq. (32). The characteristic double-layer thickness is easily calculated to be

$$\lambda_c = \lambda_D \left(\frac{r_0}{R} \right)^2 \tanh\left(\frac{h}{2\lambda_D} \right). \tag{42}$$

The variation of λ_c with platelet and salt concentrations is illustrated in Figs. 6(a) and 6(b), for two values of the plate-

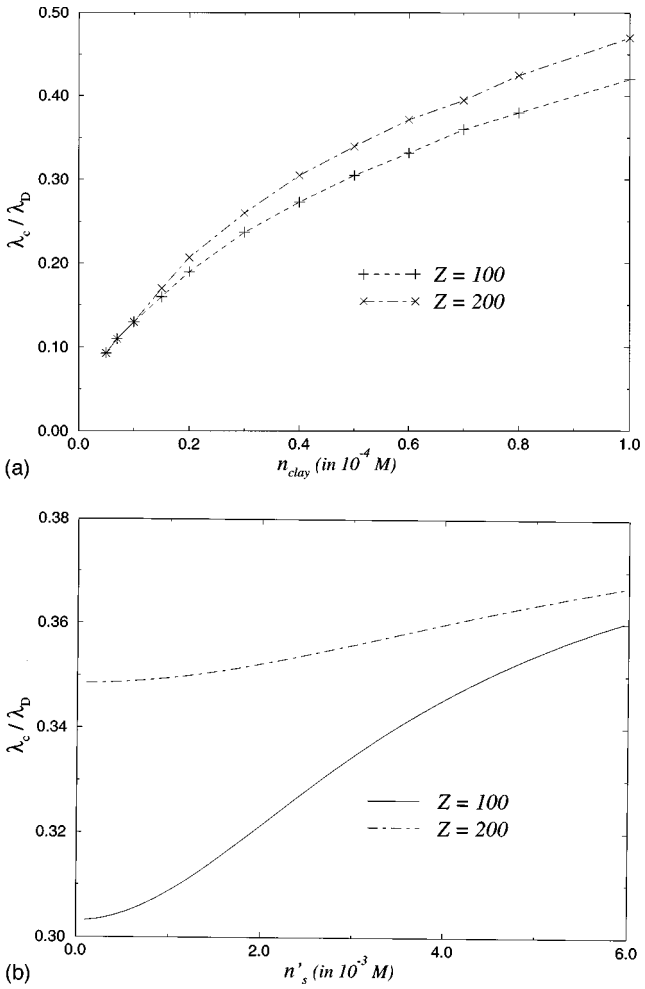

FIG. 6. (a) The characteristic double-layer thickness [see Eq. (42)] as a function of clay concentration, for the optimal aspect ratio minimizing F. The salt concentration in the reservoir is $n_s' = 10^{-3} M$. (b) Variation of the reduced double-layer thickness with salt concentration for $n = 5 \times 10^{-5} M$.

let charge. λ_c reduces to the Debye length λ_D when $r_0 \to R$ and $h \to \infty$, which corresponds to the limit of a single uniformly charged infinite plane.

Finally, as illustrated in Fig. 2, the quadrupole moment of the charge distribution inside the WS cell vanishes at the ''optimum'' ratio h/r_0, which minimizes the free energy. This coincidence is systematic and may be related to an exact result of Gruber *et al.* [21], provided the WS model yields an accurate description of a regular, periodic stacking of the platelets [17]. A partial explanation follows from the calculation given at the end of the Appendix. When the Boltzmann's weights (7) are linearized, the kinetic part of the free energy variation [cf. Eq. (A12a)] as a function of the aspect ratio is proportional to the total quadrupole [cf. Eq. (A15)]. Figure 2(b) shows this correspondance but also shows that the electrostatic part of the free energy variation, defined from Eq. (A12b), vanishes for the same aspect ratio as the kinetic one.

V. PARALLELEPIPEDIC GEOMETRY

Instead of a cylindrical WS cell, we now consider a space-filling parallelepipedic cell of dimensions $L \times L \times H$ in the x, y, and z directions, respectively (cf. Fig. 1). The potential is naturally expanded in plane waves, compatible with the periodic boundary conditions, which are equivalent to the condition of vanishing normal component of the electric field on the surface Σ bounding the prismatic WS cell:

$$\varphi(\mathbf{r}) = \sum_{\mathbf{k}} \tilde{\varphi}(\mathbf{k}) \exp\{i\mathbf{k}\cdot\mathbf{r}\}, \tag{43}$$

with

$$\mathbf{k} = 2\pi\left(\frac{n_x}{L}, \frac{n_y}{L}, \frac{n_z}{H}\right), \quad (n_x, n_y, n_z) \in \mathbb{Z}^3. \tag{44}$$

In terms of Fourier components, Eq. (10) becomes

$$(k^2 + \kappa_D^2)[\tilde{\varphi}(\mathbf{k}) - \gamma_0 \delta_{\mathbf{k},\mathbf{0}}] = \frac{4\pi}{\varepsilon} \tilde{q}_{\mathcal{P}}(\mathbf{k}), \tag{45}$$

where

$$\tilde{q}_{\mathcal{P}}(\mathbf{k}) = \frac{1}{\Omega} \int_{\Omega} q_{\mathcal{P}}(\mathbf{r}) \exp\{i\mathbf{k}\cdot\mathbf{r}\} d^3\mathbf{r}. \tag{46}$$

Consider first the case of a circular platelet (or disk) of radius r_0, as in Sec. IV; $\tilde{q}_{\mathcal{P}}(\mathbf{k})$ is easily calculated to be

$$\tilde{q}_{\mathcal{P}}(\mathbf{k}) = \frac{2\pi r_0}{k_\parallel} J_1(k_\parallel r_0), \tag{47}$$

with

$$k_\parallel = \frac{2\pi}{L}\sqrt{n_x^2 + n_y^2}.$$

The Fourier components of the electrostatic potential are then determined by substituting Eq. (47) into Eq. (45), and inverse Fourier transformation leads to the desired result:

$$\Phi(\mathbf{r}) = \beta e \varphi(\mathbf{r}) = \beta e \gamma_0 + \frac{2\pi}{b} \frac{r_0}{L^2} \sum_{(n_x, n_y) \in \mathbb{Z}^2} \frac{J_1(k_\parallel r_0)}{k_\parallel} \cos(k_x x + k_y y) \times \frac{1}{(\kappa_D^2 + k_\parallel^2)^{1/2}} \frac{\cosh[(\kappa_D^2 + k_\parallel^2)^{1/2}(h - z)]}{\sinh[h(\kappa_D^2 + k_\parallel^2)^{1/2}]}. \tag{48}$$

The resulting free energy, as calculated from the constant Debye length charging process (21) and (38), is

$$\frac{\beta}{Z} A = \frac{1}{2} \beta e \gamma_0 - \frac{4\pi}{L^2 H b} \sum_{(n_x, n_y, n_z) \in \mathbb{Z}^3} \frac{J_1^2(k_\parallel r_0)}{k_\parallel^2 (k^2 + \kappa_D^2)}. \tag{49}$$

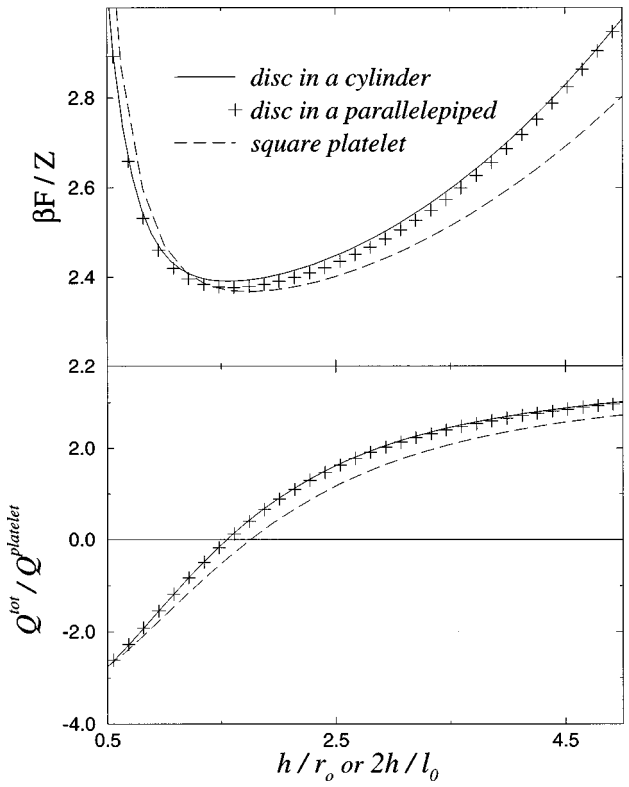

FIG. 7. Free energy and total normalized quadrupole vs h/r_0 for disks in cylindrical and parallelepipedic WS cell ($r_0=125$ Å); same quantity as a function of $H/l_0=2h/l_0$, for a square platelet of identical area and surface charge in a parallelepipedic cell ($l_0=221$ Å). The vertical lines emphasize the correlation between the minimum of the free energy and the vanishing of the total quadrupole. Here, $n_s'=10^{-3}M$, $n=2\times10^{-5}M$, and $Z=100$.

Similarly, the quadrupolar moment may be calculated from Eq. (48) to be

$$\frac{Q_{zz}^{\rm tot}}{Q_{\rm disk}}=-\frac{16}{r_0^3}\left\{\sum_{n_z=1}^{\infty}\frac{(-1)^{n_z}}{k_z^2+\kappa_D^2}r_0-\sum_{n_x=0}^{\infty}\frac{J_1(k_xr_0)}{k_x^2+\kappa_D^2}(-1)^{n_x}\frac{2}{k_x}\right\}. \tag{50}$$

The key finding is that, for given platelet and salt concentrations, the changes in free energy and quadrupole moment, induced by the change of topology of the WS cell, are practically negligible, in spite of the completely different analytical expressions [cf. Eqs. (38) and (49)], as illustrated in Fig. 7. A similar conclusion holds for the osmotic pressure calculated from Eq. (28) or the capacity evaluated from Eq. (32).

We finally consider the case of a square platelet of side l_0, within the above prismatic WS cell. In this case, the surface charge per unit area is $\sigma=-Ze/l_0^2$, while the Fourier transform of the platelet charge density is now

$$\tilde{q}_{\mathcal{P}}(\mathbf{k})=\frac{\sigma}{\Omega}\frac{4}{k_xk_y}\sin\left(\frac{k_xl_0}{2}\right)\sin\left(\frac{k_yl_0}{2}\right). \tag{51}$$

The potential is once more expanded in plane waves with the result

$$\begin{aligned}\Phi(\mathbf{r})=\beta e\varphi(\mathbf{r})=\beta e\gamma_0&\\+\frac{4}{bL^2}\sum_{(n_x,n_y)\in\mathbb{Z}^2}&\sin(k_xl_0/2)\sin(k_yl_0/2)\\\times\frac{1}{k_xk_y}&\cos(k_xx+k_yy)\frac{1}{(\kappa_D^2+k_\parallel^2)^{1/2}}\\\times\frac{\cosh[(\kappa_D^2+k_\parallel^2)^{1/2}(h-z)]}{\sinh[h(\kappa_D^2+k_\parallel^2)^{1/2}]}&.\end{aligned} \tag{52}$$

As in the case of a disk in a cylindrical WS cell, one can check from Eq. (52) that the potential goes over to that of a uniformly charged infinite plane when $l_0\to L$ [expression (37)].

The corresponding free energy is now

$$\begin{aligned}\frac{\beta}{Z}A=&\frac{1}{2}\beta e\gamma_0\\&-\frac{16}{l_0^2L^2Hb}\sum_{(n_x,n_y,n_z)\in\mathbb{Z}^3}\frac{\sin^2(k_xl_0/2)\sin^2(k_yl_0/2)}{k_x^2k_y^2(k^2+\kappa_D^2)},\end{aligned} \tag{53}$$

while the quadrupole moment reads

$$\begin{aligned}\frac{Q_{zz}^{\rm tot}}{Q_{\rm platelet}}=-\frac{48}{l_0^3}\Bigg\{&\sum_{n_z=1}^{\infty}(-1)^{n_z}\frac{l_0}{k_z^2+\kappa_D^2}\\&-2\sum_{n_x=1}^{\infty}(-1)^{n_x}\frac{\sin(k_xl_0/2)}{k_x(k_x^2+\kappa_D^2)}\Bigg\}.\end{aligned} \tag{54}$$

Explicit calculations based on these formulas lead again to results which are quite close to those obtained for circular platelets under similar physical conditions, as shown, e.g., in Fig. 7. In particular, the ''optimum'' aspect ratio is characterized by the equality of the osmotic and disjoining pressures [an expression similar to Eq. (41) holds], as illustrated in Fig. 8. However, the minima of the free energy and of the osmotic pressure do not coincide any more.

VI. INFINITE DILUTION LIMIT

The limit of very low platelet concentration n, for a fixed salt concentration n_s (or equivalently n_s'), may be derived from the expressions obtained in Secs. IV and V for prismatic geometries, by letting the volume Ω of the WS cell go to infinity. In this limit $\gamma_0=0$, and the series (36) and (48) go over to the following integral representation of the reduced potential:

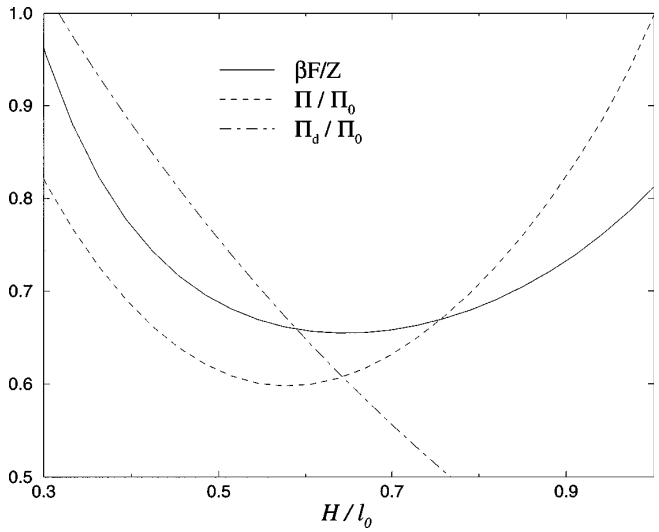

FIG. 8. Free energy, osmotic, and disjoining pressures as functions of the aspect ratio H/l_0, for a square platelet in a parallelepipedic cell. For illustrative purposes, the free energy has been shifted by an arbitrary constant along the vertical axis. The data correspond to $n=10^{-4}M$, $n_s'=10^{-3}M$, $Z=100$, and $l_0=250$ Å.

$$\Phi(r,z)=\frac{r_0}{b}\int_0^\infty dk\, J_0(kr)J_1(kr_0)\frac{e^{-\sqrt{\kappa_D^2+k^2}|z|}}{\sqrt{\kappa_D^2+k^2}}. \quad (55)$$

Along the z axis passing through the center of the disk ($r=0$), Eq. (55) reduces to

$$\Phi(r=0,z)=\frac{1}{\kappa_D b}[e^{-\kappa_D|z|}-e^{-\kappa_D\sqrt{r_0^2+z^2}}], \quad (56)$$

which goes over to the familiar exponential solution of linearized Gouy-Chapman theory in the limit $r_0\to\infty$ (infinite plane). The reduced potential at the center of the disk takes the value

$$\Phi(\mathbf{0})=\frac{e\varphi(r=0,z=0)}{k_BT}=\frac{1}{\kappa_D b}\{1-\exp(-\kappa_D r_0)\}. \quad (57)$$

This expression will be used in the concluding section to evaluate the range of validity of LPB theory.

The quadrupole moment around circular or square platelets vanishes identically in the zero concentration limit ($n\to 0$) as a consequence of the theorem by Gruber *et al.* [21].

Finally consider the problem of determining the force acting between two circular platelets (disks) $\mathcal{P}_1$ and $\mathcal{P}_2$, in the limit of vanishing concentration ($n\to 0$), and for a given salt concentration (in the limit $n\to 0$, $n_s\to n_s'$). Let $(\mathbf{r}_1,\mathbf{n}_1)$ and $(\mathbf{r}_2,\mathbf{n}_2)$ be the center positions and normals of the two disks, and let $\varphi(\mathbf{r})$ be the total electrostatic potential due to the two disks and their electric double layers; $\varphi(\mathbf{r})$ vanishes as $|\mathbf{r}|\to\infty$. In the LPB approximation, $\varphi(\mathbf{r})$ satisfies Eq. (10), with $\gamma_0=0$, and two source terms

$$(\nabla^2-\kappa_D^2)\varphi(\mathbf{r})=-\frac{4\pi}{\varepsilon}[q_{\mathcal{P}_1}(\mathbf{r})+q_{\mathcal{P}_2}(\mathbf{r})]. \quad (58)$$

Since the discontinuity of the electric field upon crossing one of the platelets [characterized by the surface charge density $q_{\mathcal{P}_\alpha}(\mathbf{r})$] is independent of the presence of the other platelet, the solution $\varphi(\mathbf{r})$ of Eq. (58) is just the superposition of the solutions for each platelet separately:

$$\varphi(\mathbf{r})=\varphi_1(\mathbf{r})+\varphi_2(\mathbf{r}). \quad (59)$$

This simple property is a consequence of the linearization, and does not hold within nonlinear PB theory. The solution of Eq. (58), and the resulting co- and counterion density profiles may now be used to calculate the pressure tensor (23) for given positions and orientations of the platelets. The force $\mathbf{F}_i$ acting on platelet i (=1 or 2) follows then from integration of $\overleftrightarrow{\Pi}$ over the two faces Σ_p^+ and Σ_p^- of the platelet:

$$\mathbf{F}_i=-\int_{\Sigma_{p,i}^+;\Sigma_{p,i}^-}\overleftrightarrow{\Pi}\cdot d\mathbf{S}_i. \quad (60)$$

Since the normal $\mathbf{n}_i=d\mathbf{S}_i/|d\mathbf{S}_i|$ has opposite orientations on the faces $\Sigma_{p,i}^+$ and $\Sigma_{p,i}^-$, the kinetic contributions $\rho^\alpha(\mathbf{r})k_BT$ to the pressure tensor (23), which are continuous across the platelet, do not contribute to the force (60). The normal component of the electric field $\mathbf{E}=-\nabla\varphi$, however, suffers a discontinuity across the uniformly charged platelet, and hence contributes to the surface integral in Eq. (60).

The total electric field $\mathbf{E}$ in the immediate vicinity of the platelet $\mathcal{P}_i$ may be decomposed into a discontinuous and a continuous part:

$$\mathbf{E}=\mathbf{E}_i^{(d)}+\mathbf{E}_i^{(c)}=\pm\frac{2\pi}{\varepsilon}\sigma\mathbf{n}_i+\mathbf{E}_i^{(c)}, \quad (61)$$

where the + and − signs go with the upper ($\Sigma_{p,i}^+$) and lower ($\Sigma_{p,i}^-$) faces, respectively. Subsituting Eq. (61) into (60) leads to the desired result:

$$\mathbf{F}_i=\sigma\int_{\Sigma_{p,i}}\mathbf{E}_i^{(c)}d^2S\,(i=1,2), \quad (62)$$

where the integration is now over the surface of the platelet. For symmetry reasons, the only nonvanishing contribution of $\mathbf{E}_i^{(c)}$ to the surface integral in Eq. (62) is the electric field due to the other platelet and its associated electric double layer. In the case of two coaxial parallel disks, the force $\mathbf{F}_1=-\mathbf{F}_2$ is along the common axis (chosen to be the z axis) and the result (55) may be used to compute the gradient of φ along Oz. The resulting force is easily cast in the form

$$F_z(d)=(\pi r_0^2)\frac{4\pi\sigma^2}{\varepsilon}\int_0^\infty J_1^2(x)\frac{1}{x}\exp\left\{-\frac{d}{r_0}\sqrt{x^2+\kappa_D^2r_0^2}\right\}dx, \quad (63)$$

where d is the distance between the two disks. For any finite salt concentration (i.e., nonvanishing κ_D), the decay of F_z with d is essentially exponential as illustrated in Fig. 9. In the limit of vanishing salt concentration ($\kappa_D\to 0$), F_z decays like a power law. For $d\gg r_0$, we find in that limit

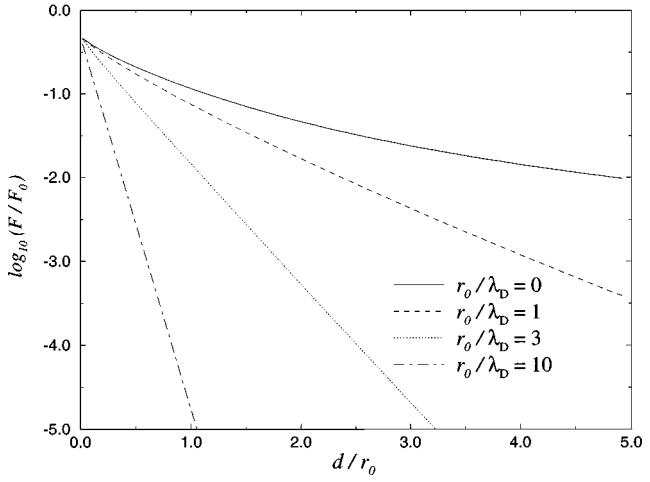

FIG. 9. Variation of the force F_z with the distance d between the centers of coaxial disks ($F_0 = 4\pi^2 r_0^2 \sigma^2/\varepsilon$). The four curves correspond to different salt concentrations.

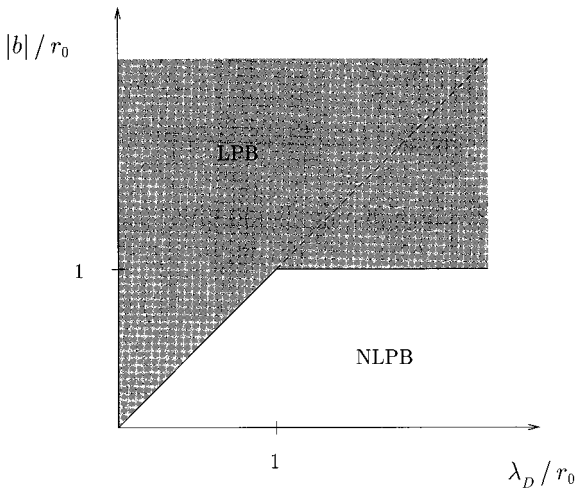

FIG. 10. Limits of validity for the linearized approximation of PB theory, for a disk of radius r_0 in the infinite dilution limit. The dashed line corresponds to the case of an infinite plane (in which case r_0 is an arbitrary normalization length). λ_D denotes the Debye length and b is the Gouy length.

$$F_z(d) \overset{d \gg r_0}{\sim} \frac{1}{\varepsilon}\left(\frac{\pi r_0^2 \sigma}{d}\right)^2 \left[1 - \frac{3r_0^2}{2d^2}\right]. \tag{64}$$

Note that the force (63) is repulsive at all distances.

VII. CONCLUSION

While most of the existing theoretical literature on suspensions of charged lamellar particles or membranes deals with the simpler one-dimensional problem of infinite charged planes, we have examined in this paper the case of stacks of finite-size, circular, or square platelets corresponding, for instance, to swollen clays. The intractable many-platelet problem is reduced to the much simpler problem of a single platelet within an electrically neutral Wigner-Seitz cell of appropriate volume and topology. The co- and counterion density profiles have been obtained from analytic solutions of linearized Poisson-Boltzmann equation with appropriate boundary conditions on the surface of cylindrical and parallelepipedic cells. The relevant characteristics of the electric double layer and the resulting thermodynamic properties have been calculated over a wide range of physical conditions. The most notable results may be summarized as follows.

(a) For a given cell volume Ω, the system selects an optimal size ratio corresponding to the minimum free energy. The selected size ratio is practically independent of the platelet charge density σ, and of the salt concentration, but varies with the macroscopic platelet concentration n.

(b) The osmotic presure Π and depletion pressure Π_d due to the co- and counterions have qualitatively different variations with the aspect ratio for fixed σ, clay, and salt concentration, but coincide at the optimum aspect ratio which minimizes the free energy. We have a simple explanation for this coincidence but not for the observation that the osmotic pressure exhibits a minimum at the same aspect ratio as the free energy, at least in the case of circular platelets.

(c) The total quadrupole moment of the charge distribution in the WS cell vanishes at the optimal aspect ratio; this observation may be related to an exact property of neutral charge distributions in thermodynamic equilibrium [21] (in the present case, the theorem applies because of exponential screening). A partial explanation of this correlation has been given at the end of Sec. IV.

The limitations of the present LPB theory must be underlined. Returning to the expression (57) of the reduced electrostatic potential at the center of an *isolated* charged disk, it is clear that linearization of the Boltzmann factors in the PB equation (8) is justified only provided $|\Phi(\mathbf{0})| \ll 1$, i.e., when $|b| > \lambda_D$ (which corresponds to the limit of low surface charge σ or high salt concentration) or $r_0 < \lambda_D$ and $r_0 < |b|$. This latter condition is rather academic for Laponite clay disks (it yields $Z < 10$). Figure 10 summarizes the limits of validity of the linearized theory for an isolated platelet. Strictly speaking, the above criteria apply in the infinite dilution limit $n \to 0$, and we may expect that they become necessary but not sufficient conditions for finite concentrations n [5], so that the shaded area in Fig. 10 should decrease. Neglecting the clay contribution to the Debye length, the criterion $\lambda_D < |b|$ yields $Z < 2.3 \times 10^{-n/2} r_0^2$, for a 10^{-n} molar monovalent salt concentration, with r_0 expressed in nanometers. In practice, we carried out calculations for $r_0 = 12.5$nm (a typical size of Laponite particles); this means that Z must be chosen less than about $400 \times 10^{-n/2}$. In fact, many of our calculations were carried out for $Z = 100$, in which case, strictly speaking, the salt concentration would have to be 10^{-1} mol or higher for LPB theory to be applicable. The case of lower salt concentration and more realistic values of Z (e.g., $Z \simeq 10^3$ for Laponite) may be solved either by numerical solutions of the full (nonlinear PB) equation or by retaining the linearized solutions presented here in conjunction with an appropriate charge renormalization procedure inspired by the treatment presented in Refs. [12] in spherical geometry. The corresponding effective charge density on the platelet might well be nonuniform. Work along these lines is in progress.

ACKNOWLEDGMENTS

Useful conversations with Marjolein Dijkstra, Paul Madden, and Thierry Biben are gratefully acknowledged.

APPENDIX

Consider the case of a charged platelet $\mathcal{P}$ confined in a WS cell with its neutralizing counterions and salt. A local change $\delta\Omega$ in volume of the cell (with or without conservation of the overall volume) changes the potential and the microion densities, but not the charge density of the platelet. The boundary conditions of vanishing normal electric field on the surface Σ of the cell are enforced during this change. It will be shown that when the total number of ions, N^α, in the cell are held constant, the free energy F changes according to Eq. (22). From Eq. (16), the change in the internal energy can be written

$$\delta U=\frac{1}{2}\int_\Omega (q\,\delta\varphi+\varphi\,\delta q)d^3\mathbf{r}+\frac{1}{2}\int_{\delta\Omega} q\varphi d^3\mathbf{r}, \qquad \text{(A1)}$$

where $q(\mathbf{r})=q_{\mathcal{P}}(\mathbf{r})+e[\rho^+(\mathbf{r})-\rho^-(\mathbf{r})]$ is the total charge density. It follows from Poisson's equation (4) and integrations by parts that

$$\int_\Omega q\,\delta\varphi d^3\mathbf{r}=\int_\Omega \varphi\,\delta q d^3\mathbf{r}+\frac{\varepsilon}{4\pi}\oint_\Sigma \varphi\nabla(\delta\varphi)\cdot d\mathbf{S}. \qquad \text{(A2)}$$

For any vector field $\boldsymbol{A}(\mathbf{r})$, the elementary variation of the flux over the surface Σ can be written

$$\delta\left(\oint_\Sigma \boldsymbol{A}\cdot d\mathbf{S}\right)=\oint_\Sigma \delta\boldsymbol{A}\cdot d\mathbf{S}+\int_{\delta\Omega}\nabla\cdot\boldsymbol{A}d^3\mathbf{r}. \qquad \text{(A3)}$$

With $\boldsymbol{A}=\varphi\nabla\varphi$, the above relation can be used to differentiate the identity

$$\oint_\Sigma \varphi\nabla(\varphi)\cdot d\mathbf{S}=0. \qquad \text{(A4)}$$

One finds

$$\frac{\varepsilon}{4\pi}\oint_\Sigma \varphi\nabla(\delta\varphi)\cdot d\mathbf{S}=\int_{\delta\Omega} q\varphi\, d^3\mathbf{r}-\frac{\varepsilon}{4\pi}\int_{\delta\Omega}(\nabla\varphi)^2 d^3\mathbf{r}, \qquad \text{(A5)}$$

so that δU can be cast in the form

$$\delta U=\int_\Omega \varphi\,\delta q\, d^3\mathbf{r}+\int_{\delta\Omega} q\varphi\, d^3\mathbf{r}-\frac{\varepsilon}{8\pi}\int_{\delta\Omega}(\nabla\varphi)^2 d^3\mathbf{r}. \qquad \text{(A6)}$$

From Eq. (17) and relation (7), the change in entropy reads

$$\delta S=k_B\sum_{\alpha=+,-}\int_{\delta\Omega}\rho^\alpha(\mathbf{r})d^3\mathbf{r}+\int_{\delta\Omega}\varphi q\, d^3\mathbf{r}+\int_\Omega \varphi\,\delta q\, d^3\mathbf{r}$$
$$-k_B\sum_{\alpha=+,-}\ln(\rho_0^\alpha\Lambda_\alpha^3)\left[\int_\Omega \delta\rho^\alpha d^3\mathbf{r}+\int_{\delta\Omega}\rho^\alpha d^3\mathbf{r}\right], \qquad \text{(A7)}$$

where it was remembered that

$$\delta q_{\mathcal{P}}(\mathbf{r})=0 \quad \text{and} \quad \int_{\delta\Omega} q_{\mathcal{P}}(\mathbf{r})\varphi(\mathbf{r})d^3\mathbf{r}=0.$$

Since $\delta N^+=\delta N^-=0$, the expression for the entropy simplifies to

$$\delta S=k_B\sum_{\alpha=+,-}\int_{\delta\Omega}\rho^\alpha(\mathbf{r})d^3\mathbf{r}+\int_{\delta\Omega}\varphi q\, d^3\mathbf{r}+\int_\Omega \varphi\,\delta q\, d^3\mathbf{r}. \qquad \text{(A8)}$$

Upon substitution of Eqs. (A6) and (A8) into $\delta F=\delta U-T\delta S$, we obtain Eq. (22),

$$\delta F=-k_BT\sum_{\alpha=+,-}\int_{\delta\Omega}\rho^\alpha(\mathbf{r})d^3\mathbf{r}-\frac{\varepsilon}{8\pi}\int_{\delta\Omega}[\nabla\varphi]^2 d^3\mathbf{r}$$
$$=-\int_{\delta\Omega}\Pi(\mathbf{r})d^3\mathbf{r}, \qquad \text{(A9)}$$

where the following local osmotic pressure was introduced:

$$\Pi(\mathbf{r})=k_BT\sum_{\alpha=+,-}\rho^\alpha(\mathbf{r})+\frac{\varepsilon}{8\pi}(\nabla\varphi)^2. \qquad \text{(A10)}$$

Near the surface Σ, the relation between $\Pi(\mathbf{r})$ and the pressure tensor (23) is

$$\Pi(\mathbf{r})=\boldsymbol{n}_\Sigma\cdot\vec{\vec{\Pi}}\cdot\boldsymbol{n}_\Sigma, \qquad \text{(A11)}$$

so that the osmotic pressure Π may be defined as the average of $\Pi(\mathbf{r})$ over the surface Σ [cf. Eq. (28)].

The variation δF can be partitioned into kinetic and electrostatic contributions

$$\delta F^{\text{kin}}=-k_BT\sum_{\alpha=+,-}\int_{\delta\Omega}\rho^\alpha(\mathbf{r})d^3\mathbf{r}, \qquad \text{(A12a)}$$

$$\delta F^{\text{el}}=-\frac{\varepsilon}{8\pi}\int_{\delta\Omega}[\nabla\varphi]^2 d^3\mathbf{r}. \qquad \text{(A12b)}$$

Within linearized PB theory, we shall finally prove that, when the shape of the cell is modified at constant total volume, the resulting variation of the free energy is proportional to the total quadrupole moment of the charge distribution inside the cell.

With the chosen boundary conditions, the total quadrupole defined from Eq. (33) is

$$Q_{zz}^{\mathrm{tot}}=\frac{\varepsilon}{2}\oint_{\Sigma}\varphi(\mathbf{r})\nabla(2z^2-x^2-y^2)\cdot d\mathbf{S}. \tag{A13}$$

Within linearized PB theory,

$$\delta F^{\mathrm{kin}}=\beta e(\rho_0^+-\rho_0^-)\int_{\delta\Omega}\varphi(\mathbf{r})d^3\mathbf{r}. \tag{A14}$$

Consider the case of a cylindrical WS cell. Taking into account the conservation of the overall volume, it is straightforward to show that

$$H\frac{\delta F^{\mathrm{kin}}}{\delta H}\bigg|_{T,\Omega,N^\alpha}=\frac{1}{2}\gamma_0\kappa_D^2 Q_{zz}^{\mathrm{tot}}. \tag{A15}$$

A similar result holds for a parallelepipedic cell.

[1] E. J. W. Verwey and J. Th. G. Overbeek, *Theory of the Stability of Lyophobic Colloids* (Elsevier, New York, 1948).
[2] G. Gouy, J. Phys. **9**, 457 (1910).
[3] D. L. Chapman, Philos. Mag. **25**, 475 (1913).
[4] S. L. Carnie and G. M. Torrie, Adv. Chem. Phys. **56**, 141 (1984).
[5] D. Andelman, in *Membranes, their Structure and Conformations*, edited by R. Lipowsky and E. Sackmann (Elsevier, Amsterdam, 1996).
[6] H. Löwen, J. P. Hansen, and P. A. Madden, J. Chem. Phys. **98**, 3275 (1993).
[7] H. Löwen and G. Kramposthuber, Europhys. Lett. **23**, 673 (1993).
[8] J. C. Crocker and D. G. Grier, Phys. Rev. Lett. **73**, 352 (1994).
[9] R. M. Fuoss, A. Katchalsky, and S. Lifson, Proc. Acad. Sci. U.S.A. **37**, 579 (1951).
[10] J. L. Barrat and J. F. Joanny, Adv. Chem. Phys. **94**, 1 (1996).
[11] For recent reviews, see R. Evans, in *Fundamentals of Inhomogeneous Fluids*, edited by D. Henderson (Marcel Dekker, New York, 1992); or J. P. Hansen and E. Smargiassi, in *Monte Carlo and Molecular Dynamics of Condensed Matter Systems*, edited by K. Binder and G. Ciccotti (SIF, Bologna, 1996).
[12] S. Alexander, P. M. Chaikin, P. Grant, G. J. Morales, P. Pincus, and D. Hone, J. Chem. Phys. **80**, 5776 (1984); J. D. Groot, *ibid.* **95**, 9191 (1991).
[13] H. van Olphen, *Clay Colloid Chemistry*, 2nd ed. (John Wiley, New York, 1977).
[14] Laporte Inorganics, Laponite Technical Bulletin No. L104/90/A (unpublished).
[15] J. P. Hansen and E. Trizac, Physica A **235**, 257 (1997).
[16] E. Trizac and J. P. Hansen, J. Phys., Condens. Matter **8**, 9191 (1996).
[17] E. Trizac and J. P. Hansen, J. Phys., Condens. Matter **9**, 2683 (1997).
[18] R. B. Secor and C. J. Radke, J. Colloid Interface Sci. **103**, 237 (1985); F. R. C. Chang and G. Sposito, *ibid.* **163**, 19 (1994).
[19] R. A. Marcus, J. Chem. Phys. **23**, 1057 (1955).
[20] L. D. Landau and E. M. Lifschitz, *Electrodynamics of Continuous Media* (Pergamon Press, Oxford, 1984).
[21] Ch. Gruber, J. L. Lebowitz, and P. A. Martin, J. Chem. Phys. **75**, 944 (1981).
[22] M. Dubois, T. Zemb, L. Belloni, A. Delville, P. Levitz, and R. Setton, J. Chem. Phys. **96**, 2278 (1992).